HHS Public Access

Author manuscript

Nat Genet. Author manuscript; available in PMC 2017 August 27.

Published in final edited form as:

Nat Genet. 2017 April ; 49(4): 606–612. doi:10.1038/ng.3804.

Biallelic Mutations In Human *DCC* Cause Developmental Split Brain Syndrome

Saumya S. Jamuar[1,2,3,4,5,22], **Klaus Schmitz-Abe**[1,2,4,22], **Alissa M. D'Gama**[1,4,5], **Marie Drottar**[6], **Wai-Man Chan**[5,7,8], **Maya Peeva**[6,7,8], **Sarah Servattalab**[1,4,5], **Anh-Thu N. Lam**[1,4,5], **Mauricio R. Delgado**[9,10], **Nancy J. Clegg**[9], **Zayed Al Zayed**[11], **Mohammad Asif Dogar**[12], **Ibrahim A. Alorainy**[13], **Abdullah Abu Jamea**[13], **Khaled Abu-Amero**[14], **May Griebel**[15], **Wendy Ward**[15], **Ed S. Lein**[16], **Kyriacos Markianos**[1,2,4,17], **A. James Barkovich**[18], **Caroline D. Robson**[19], **P. Ellen Grant**[6,19], **Thomas M. Bosley**[20], **Elizabeth C. Engle**[1,4,5,7,8,21], **Christopher A. Walsh**[1,2,4,5,7,21], and **Timothy W. Yu**[1,2,21,*]

[1]Division of Genetics and Genomics, Boston Children's Hospital, Boston, MA, USA

[2]Department of Pediatrics, Harvard Medical School, Boston, MA, USA

[3]Department of Paediatrics, KK Women's and Children's Hospital, Paediatric Academic Clinical Programme, Duke-NUS Graduate School of Medicine, Singapore, Singapore

[4]Manton Center for Orphan Disease Research, Boston Children's Hospital, Boston, MA, USA

[5]Howard Hughes Medical Institute, Boston Children's Hospital, Boston, MA, USA

[6]Fetal-Neonatal Neuroimaging and Developmental Science Center, Division of Newborn Medicine, Boston Children's Hospital, Boston, MA, USA

[7]Department of Neurology, Boston Children's Hospital, and Harvard Medical School, Boston, MA, USA

[8]Department of Ophthalmology, Boston Children's Hospital, and Harvard Medical School, Boston, MA, USA

[*]Corresponding author: Timothy W. Yu, MD, PhD, 300 Longwood Avenue, Boston Children's Hospital, Boston, MA, 02115, USA, Phone: +1-617-919-2923, Fax: +1-617-919-2010, timothy.yu@childrens.harvard.edu.

[22]These authors contributed equally to this work

AUTHOR CONTRIBUTIONS

S.S.J., E.C.E, C.A.W., and T.W.Y. designed experiments. K.S.A. and K.M. performed the homozygosity and CNV analysis. S.S.J., A.M.D., A-N.T.L., and S.S.J. performed the ddPCR, junction PCR and RT-PCR. C.W.M. performed Sanger sequencing of Family 2. M.P., M.D., E.G. performed the DTI and tractography analyses. M.R.D., N.J.C, M.G., Z.A.Z., M.A.S., A.A.J., K.A.A., T.M.B. performed the phenotypic assessment of the patients, A.J.B., C.A.W., M.D., M.P., C.D.R., I.A.A., E.G., E.C.E., and T.W.Y. reviewed the MRI imaging studies. S.S.J., E.C.E., C.A.W., and T.W.Y. wrote the manuscript. All co-authors reviewed and approved the final version of the submitted manuscript.

COMPETING FINANCIAL INTEREST

The authors disclose that T.W.Y. is co-founder of Claritas Genomics, a gene diagnostic and genomic medicine company, and S.S.J. is co-founder of Global Gene Corporation Pte Ltd, a gene diagnostic company; however, T.W.Y. and S.S.J. declare no competing financial interests related to the publication of this work. The remaining authors do not have any financial conflict of interest that might be construed to influence the results or interpretation of this work.

DATA AVAILABILITY STATEMENT

Supporting genotype and DTI data from this study are available from the corresponding author upon request. Variant data from the families presented here has been deposited in ClinVar (Accession XXXXX; http://XXXXXX) [submission in process].

[9]Department of Neurology, Texas Scottish Rite Hospital for Children, Dallas, TX, USA

[10]Department of Neurology and Neurotherapeutics, University of Texas Southwestern Medical Center at Dallas, Dallas, TX, USA

[11]Department of Orthopedic Surgery, King Faisal Specialist Hospital and Research Centre, Riyadh, Saudi Arabia

[12]Imaging Institute, Cleveland Clinic, Abu Dhabi, UAE

[13]Department of Radiology, King Saud University, Riyadh, Saudi Arabia

[14]Department of Ophthalmology, King Saud University, Riyadh, Saudi Arabia

[15]Department of Pediatrics and Neurology, The Arkansas Children's Hospital and The University of Arkansas for Medical Sciences, Little Rock, AR, USA

[16]Allen Institute for Brain Science, Seattle, Washington, USA

[17]Department of Pathology, Harvard Medical School, Boston, MA, USA

[18]Department of Radiology and Biomedical Imaging, University of California, San Francisco, CA, USA

[19]Department of Radiology, Boston Children's Hospital, and Harvard Medical School, Boston, MA, USA

[20]The Wilmer Eye Institute, Johns Hopkins University, Baltimore, MD, USA and Dept of Ophthalmology, College of Medicine, King Saud University, Riyadh, Saudi Arabia

[21]Program in Medical and Population Genetics, Broad Institute of Massachusetts Institute of Technology (MIT) and Harvard, Cambridge, MA, USA

Abstract

Motor, sensory, and integrative activities of the brain are coordinated by a series of midline-bridging neuronal commissures whose development is tightly regulated. Here we report a novel human syndrome in which these commissures are widely disrupted, causing clinical manifestations of horizontal gaze palsy, scoliosis, and intellectual disability. Affected individuals were found to possess biallelic loss-of-function mutations in the axon guidance receptor *Deleted in Colorectal Carcinoma* (*DCC*), a gene previously implicated in congenital mirror movements when mutated in the heterozygous state, but whose biallelic loss-of-function human phenotype has not been reported. Structural MRI and diffusion tractography demonstrated broad disorganization of white matter tracts throughout the human CNS including loss of all commissural tracts at multiple levels of the neuraxis. Combined with data from animal models, these findings show that *DCC* is a master regulator of midline crossing and development of white matter projections throughout the human CNS.

Commissural neurons are responsible for bridging the left and right halves of the central nervous system, and are hypothesized to account for the emergence of key neurobiological features during vertebrate evolution such as depth perception and locomotion. Disruption of subsets of brain commissures occurs in a number of human syndromes: in the forebrain,

agenesis of the corpus callosum (ACC), the largest commissural tract in the human brain, may be seen as an isolated feature or in combination with other malformations (*e.g.*, holoprosencephaly)[1–4], with or without intellectual disability. In the brainstem, disruption of midbrain and pontine commissural tracts is a key feature of the genetic syndrome horizontal gaze palsy with progressive scoliosis (HGPPS [MIM: 607313]) due to biallelic mutations in *ROBO3* [MIM: 608630])[5]. Individuals with HGPPS exhibit abnormalities of conjugate eye movement and early onset scoliosis, but normal intellect. In this report, we describe a new human genetic syndrome that combines features of ACC with HGPPS. Affected individuals exhibit clinical manifestations of horizontal gaze palsy, intellectual disability and scoliosis (Fig. 1, Supplementary Fig. 1). We trace the cause of this syndrome to biallelic mutations in the axon guidance receptor *Deleted in Colorectal Carcinoma (DCC* [MIM: 120470]), a gene previously implicated via heterozygous mutations in congenital mirror movements[6–8], but whose human knockout phenotype has not been described.

Family 1 was from Mexico. Two boys suffered from a constellation of neurologic abnormalities including horizontal gaze palsy, intellectual disability, and progressive scoliosis (Supplementary Table 1; Fig. 2a, Supplementary note). MR brain imaging revealed a number of abnormalities in the affected individuals (Supplementary Table 1, Fig. 1, Supplementary Fig. 1), including ACC and absence of the anterior (AC) and hippocampal commissures (HC). The massa intermedia was slightly large, possibly indicative of partial fusion of the thalamus, although normal variation could not be excluded. Pons and midbrain structures were hypoplastic, and there was a large midline cleft throughout the extent of the brainstem contributing to a butterfly shaped medulla (Supplementary Table 1, Supplementary Fig. 1b–g).

Family 2 was from Saudi Arabia. Parents were first cousins, and had a daughter affected with horizontal gaze palsy, developmental delay and progressive scoliosis (Supplementary Table 1, Fig. 2b, Supplementary note). MR imaging of the brain demonstrated ACC and a large midline cleft of the brainstem (Fig. 1f–i), resembling abnormalities seen in Family 1.

Homozygosity mapping in Family 1 revealed a large 23 cM block of homozygosity on chromosome 18 that was shared by both affected individuals (Supplementary Fig. 2a). CNV analysis demonstrated that this region contained two homozygous deletions of ~36 kb and ~7 kb at 18q12.3 and 18q21.2, respectively (Supplementary Fig. 3). The 18q12.3 deletion did not overlap any known genes, and is a site of frequent copy number variation in the population (DGV esv2421793, deletion observed in 1.5% of HapMap samples). In contrast, the 7kb 18q21.2 deletion was absent from public or internal databases, and was predicted to lie within the gene *DCC* (Supplementary Fig. 3). *DCC* encodes a 1447 amino acid cell surface receptor with four immunoglobulin and six fibronectin type III repeats, a transmembrane domain, and an intracellular domain[9]. DCC acts as a receptor for Netrin[10], a diffusible guidance cue expressed at the CNS midline; together, DCC and Netrin constitute key members of a signaling pathway for axon guidance that is evolutionarily conserved from *C. elegans* through vertebrates[11]. In humans, heterozygous mutations in *DCC* have been shown[6] to cause congenital mirror movements (CMM/MRMV1 [MIM: 157600]), an autosomal dominant condition in which intentional movements on one side of the body are accompanied by involuntary, pathological movements on the opposite side. Besides mirror

movements, described patients with heterozygous *DCC* mutations are otherwise neurotypical, lacking neurocognitive symptoms, eye movement abnormalities, scoliosis, or brain malformations. To our knowledge, no patients with biallelic mutations in *DCC* have been described to date.

Digital droplet PCR confirmed the homozygous *DCC* deletion in both affected boys. Their mother was a heterozygous carrier, and their father was unavailable for analysis (Supplementary Fig. 4a). A series of PCR probes (Supplementary Fig. 4b) was used to localize the precise breakpoint (Supplementary Fig. 4c), revealing a 7682 bp deletion (Fig. 2d). This deletion removed the 3′ end of exon 1, containing 61 bp of *DCC* coding sequence (NM_005215.3) and 7.6 kb of intronic sequence (Fig. 2d). RT-PCR from patient lymphoblasts demonstrated that this deletion causes exon 1 to be skipped entirely (Supplementary Fig. 5a–c). Exon 1 is the first coding exon and contains the signal peptide, required for correct orientational insertion into the membrane, and part of the first of DCC's four immunoglobulin repeats, which adopt a horseshoe configuration critical for netrin-mediated guidance[12]. Disruption of these features strongly predicts that this mutation represents a functional null.

Targeted sequencing of *DCC* in the proband of Family 2 revealed a homozygous 7 bp deletion in exon 4 (c.788_794delTTTCTGG) (Fig. 2e). Both parents were carriers. This variant was absent from public databases (Exome Aggregation Consortium, Exome Variant Server, dbSNP146, 1000 Genomes Project) as well as an internal exome database of >1000 Middle Eastern samples. It is at amino acid position 263 (of 1447) in the third immunoglobulin repeat, resulting in frameshift and premature termination 36 amino acids downstream (p.Val263Alafs*36).

We sequenced coding regions of *DCC* in 33 additional patients with abnormalities of the corpus callosum, but not known to have horizontal gaze palsy or scoliosis. Only a few heterozygous missense changes of uncertain significance were detected, and the four patients involved were subsequently found to have plausible alternative explanations for their callosal abnormalities (Supplementary Table 2). No additional biallelic coding mutations were found (Supplementary Table 2), indicating that biallelic mutations in *DCC* are not common causes of ACC in general. *DCC* sequencing in a cohort of 31 patients with ACC plus interhemispheric cyst did reveal one individual (Family 3, individual II:1; Supplementary Table 1, Fig. 2c, Supplementary note) with a homozygous missense variant (c.2071C>A, p.Gln691Lys) (Fig. 2f) affecting the third fibronectin repeat. In a previously published description of this individual (Patient 8)[13], he was noted to have ACC, interhemispheric cyst, and modest intellectual deficits. No information about eye movement abnormalities, mirror movements, or scoliosis was available, and he was unfortunately not available for recontact. This variant is not found in public allele frequency databases, nor have any other variants affecting this amino acid position been reported. p.Gln691Lys alters a glutamine residue in the third fibronectin (FN) type III domain that is highly evolutionarily conserved (Fig. 2g), and this change was predicted to be deleterious by 5/7 algorithms applied (Supplementary Tables 3 and 4). This finding suggests that weaker biallelic mutations in *DCC* may cause milder phenotypes, although additional cases will be required to confirm this.

MR diffusion imaging was available for the affected individual from Family 2. We therefore performed diffusion tractography to reconstruct white matter tracts from this individual. In age-matched control individuals, whole brain tractography and fractional anisotropy maps reveal a highly organized network of fibers, distinguishable as associational (cortical-cortical projections), commissural (interhemispheric projections), and subcortical fibers (descending projections). In contrast, tractography of the *DCC(−/−)* brain revealed striking abnormalities (Fig. 3, Supplementary Fig. 6, Supplementary Fig. 7, Supplementary Movies). In place of the normal pattern of interdigitating callosal fibers, no commissural tracts were evident, either on tractography or FA maps (Fig. 3a–b, Supplementary Fig. 7a). *DCC(−/−)* reconstructions did reveal characteristic, longitudinally misguided Probst bundles along the lateral ventricles (Supplementary Fig. 7b), a classic finding in some individuals with agenesis of the corpus callosum[14]. White matter tracts in the *DCC(−/−)* mutant brain were much more disorganized than in control individuals (Fig. 3a–b, Supplementary Fig. 7a). Fewer fibers could be reconstructed, and those tracts that could showed much lower anisotropy, a measure of axonal integrity and myelination (Fig. 3a–b, Supplementary Fig. 6). This effect was not limited to commissural fibers, but was strongly evident in associational and subcortical fibers as well. FA maps pseudocolored for directionality (Fig. 3a–b) suggested the *DCC(−/−)* brain to be especially depleted of associational fiber bundles (*e.g.* projecting longitudinally or anterior-posterior, encoded green), with fibers instead predominantly arranged in a radial fashion (*e.g.* dorsal-ventral, encoded blue). In comparison, whole brain tractography of a patient with idiopathic agenesis of the corpus callosum (Fig. 3a–b, Supplementary Fig. 6) did not show similar disorganization, reduced fiber number, or low anisotropy, suggesting that these are neuroanatomic features specific to disruption of *DCC*.

Patients with HGPPS do not exhibit ACC but have been shown to have distinctive crossing abnormalities in the brainstem, including the absence of major pontine crossing fiber tracts and lack of decussation of the superior cerebellar peduncles (SCPs) in the midbrain[15]. Color FA maps from our *DCC(−/−)* patient showed a similar failure of SCPs to decussate, as evidenced by absence of the typical midbrain “red dot” sign[16] (Fig. 3c). In the pons, our patient had small middle cerebellar peduncles and also lacked evidence of transverse pontine fibers (Fig. 3c), like patients with HGPPS.

Heterozygous mutations in *DCC* in humans have been associated with CMM[6–8], and include several early truncating mutations (Fig. 5a), arguing that the relevant underlying mechanism is loss of function via haploinsufficiency. The *DCC* mutations described in this report are also predicted to be loss of function, but none of the heterozygous carriers (that could be assessed) were reported to exhibit mirror movements. Furthermore, while the proband in Family 1 exhibited mirror movements, the affected individuals in Family 2 and 3 did not. The reason for this variability is unclear, but incomplete penetrance is seen in CMM as well[6], and it is possible that this phenotype may be influenced by additional, as yet uncharacterized, background genetic modifier effects. It is also possible that involuntary mirror movements require a particular mix of contralateral and ipsilateral connectivity due to partial loss of *DCC* function (e.g., heterozygous knockout), but which may be lacking in a complete knockout. We note for example that patients with biallelic *ROBO3* mutations

exhibit uncrossed ascending sensory and descending motor pathways, and also lack mirror movements.

In embryonic mouse brain, *DCC* is highly expressed in telencephalic cortical plate as well as in developing brainstem nuclei (Fig. 4)[10]. Netrin-1 (*Ntn-1*) is expressed in ventral midline structures of the developing forebrain and third and fourth ventricles (Fig. 4)[17], and similar findings have been recently reported in postmortem human fetal tissue[18]. The forebrain crossing deficits observed in our patients are reminiscent of abnormalities previously reported in mouse knockout models of *Netrin-1* or *DCC* deficiency, which are also acallosal[19–21]. This is thought to be due to failure of *DCC* signaling in pioneering commissural axons from the cingulate and neocortex[22,23]. Crossing deficits in the brainstem are less consistently predicted from animal studies, although zebrafish *DCC* mutants show hindbrain startle circuit abnormalities, and tract positioning defects have been observed in mice[22,23]. Animal studies have also implicated *DCC* in the formation of a wide variety of additional axon tracts, including corticospinal tract development in mice[21], axon guidance in the olfactory bulb[24], and patterning of thalamocortical projections[25,26]. *DCC* and *Netrin-1* have also been shown to play a role in oligodendrocyte myelin regulation[27,28], potentially corresponding to the loss of tract fiber integrity on DTI imaging observed here.

The human *DCC* knockout phenotype appears to unify major clinical and neuroimaging features of three separate disorders of axon guidance, ACC, HGPPS, and CMM (previously associated with heterozygous mutations in *DCC*[6]) (Fig. 5b–c). Individuals with *DCC*(−/−) mutations have brainstem flattening/midline clefting and eye movement abnormalities similar to those seen in HGPPS[5,14], reflecting shared brainstem crossing defects disrupting pathways controlling conjugate gaze. They also share progressive scoliosis, the cause of which is less well understood. We speculate that scoliosis may pertain to unbalanced paraspinal muscle activity due to defective spinal interneuron circuits (required for coordination of left-right locomotory patterns), since these circuits have been shown to be disrupted in *Netrin-1* and *DCC*-deficient mice[29,30]. Intellectual disability is not seen in HGPPS, but can (though not always) accompany ACC[31]. Our patients' cognitive deficits may at least partially be attributable to non-commissural forebrain white matter abnormalities as well.

The overlap of the human *DCC* knockout phenotype with HGPPS is mechanistically significant. HGPPS is caused by mutations in the *ROBO3* gene, an axon guidance receptor known to interact molecularly with *DCC*[32]. *ROBO3* is a divergent mammalian homolog of the *roundabout* genes in *C. elegans*, *Drosophila*, and zebrafish. It is expressed by commissural axons of the spinal cord and hindbrain, and is required for hindbrain axon midline crossing[5]. Unlike other Robo receptors, Robo3 does not bind with high affinity to Slits and hence, does not mediate repulsion of neurons away from the midline. Instead, Robo3 forms a direct molecular complex with DCC that silences repulsion from Slits[33] (allowing developing neurons to approach) and enhances attraction to Netrins[33,34]. The similarity in the brainstem phenotypes of HGPPS and the *DCC*(−/−) patients reported here provides strong evidence that this functional hierarchy is conserved in humans as well.

In summary, this is the first human report of biallelic mutations in *DCC* in association with a novel genetic syndrome of horizontal gaze palsy, scoliosis, ACC and midline brainstem cleft. Our data demonstrate that *DCC* is essential for both forebrain and brainstem midline crossing in the human CNS. Based on our findings, we would recommend screening individuals with horizontal gaze palsy, scoliosis, ACC, and midline brainstem malformations for mutations in *DCC.* Strong consideration should also be given to other genes in the *Netrin*/*DCC* pathway as candidate genes. Further delineation of the developmental consequences of mutations in this pathway will help shed light on the evolution of bilateral symmetry in the human nervous system.

ONLINE METHODS

Standard protocol approvals and patient consents

The families reported herein provided informed consent for their participation in this research, which was conducted according to protocols approved by the institutional review boards of Boston Children's Hospital and Beth Israel Deaconess Medical Center, Boston, USA.

SNP genotyping and copy number analyses

DNA was extracted from blood using DNeasy Blood and Tissue Kit (Qiagen Inc., Valencia, CA). Genome-wide SNP screening on the two affected individuals from Family 1 was performed using Affymetrix 6.0 SNP Array (Affymetrix, USA). SNP genotyping data was used to perform homozygosity and copy number analyses. Homozygosity mapping was performed as previously described[35]. CNV analysis was performed using four algorithms in parallel (Birdsuite, PennCNV, Nexus and Affymetrix Genotyping Console), requiring a minimum of 10 probes and the concordance of at least two algorithms for specificity. To distinguish rare from common variation, results were matched against a catalog of reference CNVs generated via the same pipeline, using 1251 samples from the HapMap project (11 subpopulations, public release #3). For additional stringency, CNVs were further matched with CNVs present in the Database of Genomic Variants (DGV) as well as an internal database of CNVs from over 12000 unrelated research samples (including >1000 from the Middle East with a variety of neurodevelopmental conditions, and >105 healthy Saudi individuals).

CNV confirmation and characterization

CN predictions were confirmed using digital qPCR using predesigned probes (Life Technologies, Grand Island, NY) on the QX100 Droplet Digital PCR System (BioRad Laboratories, Hercules, CA). The boundaries of the deletion in Family 1 were determined using staggered, nested PCR primers (Integrated DNA Technologies, Inc., Coralville, Iowa) (Supplementary Table 5) spanning the predicted copy number change (Supplementary Fig. 3b).

RT-PCR of patient cell lines

To further define the effects of this deletion in the *DCC* locus, we prepared RNA from lymphoblastoid cell lines generated from an affected individual and a healthy control

(RNeasy Mini kit, Qiagen Inc, Valencia, CA). cDNA was then prepared (SuperScript III Reverse Transcriptase, Life Technologies, Grand Island, NY), and subject to RT-PCR with primers (Integrated DNA Technologies, Inc., Coralville, Iowa) designed to target different exons of the predicted *DCC* mRNA transcript (Supplementary Table 6).

Sanger sequencing to identify additional families

We performed Sanger sequencing of *DCC* (RefSeq Accession: NM_005215.3) coding regions in 64 additional families with ACC with primers designed to target all 29 exons (Supplementary Table 7).

MR Imaging and Diffusion Tensor Tractography (DTT)

MR imaging data for patient II:1 Family 2 were acquired on 1.5T scanner (GE Signa HDxt; T1: TR 500ms, TE 10 ms, voxel size: 0.7813×0.7813, slice thickness = 5mm; DTI: TR/TE = 6800/133 ms; b=800 s/mm^2, b0=1:,25 gradient directions, 1.0156 × 1.0156 in plane resolution, 5 mm slice thickness, 27 slices). Patient imaging was compared to an age matched female control and an age -matched female subject with agenesis of the corpus callosum (Isolated ACC), but no DCC mutation (3.0T Siemens TrioTim; T1: TR = 2530 ms, TE = 1.66 ms, 1mm isotropic scan; DTI: TR/TE 8000/104 ms; b=1000 s/mm^2, b0= 10 (only one of which was used for subsequent analysis to match the patient data), 30 diffusion directions, 1.1724 × 1.1724 in-plane resolution, 5mm slice thickness, 28 slices. Before image post-processing the gradient directions (gd) in the control images and isolated ACC subject were down-sampled from 30gd to 25gd to match the patient's imaging.

Data analysis and interpretation were performed at Boston Children's Hospital, Boston, MA. The diffusion data were post processed using the interpolated streamline algorithm in the Diffusion Toolkit developed at the Athinoula A. Martinos Center for Biomedical Imaging, Department of Radiology, Massachusetts General Hospital (Ruopeng Wang, Van J. Wedeen, TrackVis.org; http://trackvis.org). Diffusion tensor estimation, fractional anisotropy (FA) metrics and fiber tract reconstruction were performed using the standard linear least-squares fitting method. Fiber tracts were terminated either when the angle between two consecutive orientation vectors was greater than the given threshold of 45° or when fibers extended outside of the brain surface. The resulting tracts were displayed as either a directional fiber map or a scalar fractional anisotropy (FA) map on a 3D workstation. The color-coding of fibers based on a standard RGB directional map and describes the fiber orientation. (red fibers: left-right; green fibers: anterior-posterior, ; and blue fibers: superior-inferior). A whole brain scalar image was also calculated for each case using the fractional anisotropy (FA) scale from 0–1 and pseudocolored yellow to red. Yellow areas show isotropic diffusion indicating more random water motion and less white matter organization while red areas show the diffusion anisotropy as is normally seen along more organized (and likely myelinated) white matter tracts. The scalar map describes the magnitude of the diffusion direction in the whole brain tracts.

In Situ Hybridization (ISH)

ISH data was generated as part of the Allen Developing Mouse Brain atlas[36]. Briefly, a high-throughput ISH platform described in detail previously[37] was used to analyze transcript

distributions for *DCC* and *Netrin-1* across four embryonic ages (days postconception: E11.5, E13.5, E15.5, and E18.5), with the following adaptations: 1) addition of the nuclear Feulgen-HP Yellow counterstain to allow identification of anatomical structures and enhance ability to localize ISH signal; 2) changes in tissue embedding processes for embryonic tissue; 3) adjusted proteinase K concentrations optimized for each age; and 4) adjusted Nissl protocols for some time points. Slides were scanned using either the Image Capture System (ICS) platform developed for the Allen Mouse Brain Atlas[37] or a ScanScope® automated slide scanner (Aperio Technologies, Vista, CA) equipped with a 20× objective and Spectrum software, and whole slide images were downsampled to a resolution of 1.0 μm/pixel. Following imaging, individual section images were combined into a single slide image, and a tissue detection algorithm assigned bounding boxes to individual tissue sections. A segmentation algorithm created the expression mask, which is provided as a colorized view of expression levels across the tissue[36].

Statistics

Formal statistical testing was not applicable for the results reported.

Supplementary Material

Refer to Web version on PubMed Central for supplementary material.

Acknowledgments

We thank A Rozzo, J Partlow, B Barry and R Hill for logistical and administrative assistance, C Carruthers, research assistant in FNNDSC, for creating and compressing the DTT movie files, and H Somhegyi for her expert illustrations. We thank the individuals and their families reported herein for their participation in this research. This research was supported in part by the Repository Core for Neurological Disorders, Department of Neurology, Boston Children's Hospital, and the IDDRC (NIH P30HD018655). S.S.J. is supported by the National Medical Research Council, Singapore and Singhealth-Duke NUS Paediatric Academic Programme Nurturing Clinician Scientist Scheme. A.M.D. is supported by the National Institute of General Medical Sciences (T32GM07753) and the National Institutes of Health Ruth L. Kirschstein National Research Service Award (5T32 GM007226-39). E.C.E. contributions to this work were supported by NEI R01EY12498, IDDRC grant P30 HD018655, and the Manton Center for Orphan Disease Research. C.A.W. is supported by grants from the National Institute of Mental Health (R01MH083565), the National Institute of Neurological Disorders and Stroke (R01NS032457 and R01NS035129), the Simons Foundation, and the Manton Center for Orphan Disease Research. C.A.W. and E.C.E are Investigators of the Howard Hughes Medical Institute. T.W.Y. contributions to this work were supported by grants from the National Institute of Mental Health (R01MH083565), the Simons Foundation, and the Nancy Lurie Marks Foundation.

References

1. Edwards TJ, Sherr EH, Barkovich AJ, Richards LJ. Clinical, genetic and imaging findings identify new causes for corpus callosum development syndromes. Brain. 2014; 137:1579–613. [PubMed: 24477430]
2. Izzi L, Charron F. Midline axon guidance and human genetic disorders. Clinical genetics. 2011; 80:226–34. [PubMed: 21692777]
3. Nugent AA, Kolpak AL, Engle EC. Human disorders of axon guidance. Current opinion in neurobiology. 2012; 22:837–43. [PubMed: 22398400]
4. Van Battum EY, Brignani S, Pasterkamp RJ. Axon guidance proteins in neurological disorders. The Lancet Neurology. 2015; 14:532–46. [PubMed: 25769423]
5. Jen JC, et al. Mutations in a human ROBO gene disrupt hindbrain axon pathway crossing and morphogenesis. Science. 2004; 304:1509–13. [PubMed: 15105459]

6. Srour M, et al. Mutations in DCC cause congenital mirror movements. Science. 2010; 328:592. [PubMed: 20431009]
7. Depienne C, et al. A novel DCC mutation and genetic heterogeneity in congenital mirror movements. Neurology. 2011; 76:260–4. [PubMed: 21242494]
8. Meneret A, et al. Congenital mirror movements: mutational analysis of RAD51 and DCC in 26 cases. Neurology. 2014; 82:1999–2002. [PubMed: 24808016]
9. Kolodziej PA, et al. frazzled encodes a Drosophila member of the DCC immunoglobulin subfamily and is required for CNS and motor axon guidance. Cell. 1996; 87:197–204. [PubMed: 8861904]
10. Keino-Masu K, et al. Deleted in Colorectal Cancer (DCC) encodes a netrin receptor. Cell. 1996; 87:175–85. [PubMed: 8861902]
11. Moore SW, Tessier-Lavigne M, Kennedy TE. Netrins and their receptors. Advances in experimental medicine and biology. 2007; 621:17–31. [PubMed: 18269208]
12. Chen Q, et al. N-terminal horseshoe conformation of DCC is functionally required for axon guidance and might be shared by other neural receptors. J Cell Sci. 2013; 126:186–95. [PubMed: 23038776]
13. Griebel ML, Williams JP, Russell SS, Spence GT, Glasier CM. Clinical and developmental findings in children with giant interhemispheric cysts and dysgenesis of the corpus callosum. Pediatric neurology. 1995; 13:119–24. [PubMed: 8534276]
14. Wahl M, Barkovich AJ, Mukherjee P. Diffusion imaging and tractography of congenital brain malformations. Pediatric radiology. 2010; 40:59–67. [PubMed: 19937239]
15. Sicotte NL, et al. Diffusion tensor MRI shows abnormal brainstem crossing fibers associated with ROBO3 mutations. Neurology. 2006; 67:519–21. [PubMed: 16894121]
16. Kweldam CF, et al. Undecussated superior cerebellar peduncles and absence of the dorsal transverse pontine fibers: a new axonal guidance disorder? Cerebellum. 2014; 13:536–40. [PubMed: 24771489]
17. Serafini T, et al. Netrin-1 is required for commissural axon guidance in the developing vertebrate nervous system. Cell. 1996; 87:1001–14. [PubMed: 8978605]
18. Harter PN, et al. Spatio-temporal deleted in colorectal cancer (DCC) and netrin-1 expression in human foetal brain development. Neuropathology and applied neurobiology. 2010; 36:623–35. [PubMed: 20609112]
19. Fazeli A, et al. Phenotype of mice lacking functional Deleted in colorectal cancer (Dcc) gene. Nature. 1997; 386:796–804. [PubMed: 9126737]
20. Fearon ER, et al. Identification of a chromosome 18q gene that is altered in colorectal cancers. Science. 1990; 247:49–56. [PubMed: 2294591]
21. Finger JH, et al. The netrin 1 receptors Unc5h3 and Dcc are necessary at multiple choice points for the guidance of corticospinal tract axons. The Journal of neuroscience. 2002; 22:10346–56. [PubMed: 12451134]
22. Fothergill T, et al. Netrin-DCC signaling regulates corpus callosum formation through attraction of pioneering axons and by modulating Slit2-mediated repulsion. Cerebral cortex. 2014; 24:1138–51. [PubMed: 23302812]
23. Srivatsa S, et al. Unc5C and DCC act downstream of Ctip2 and Satb2 and contribute to corpus callosum formation. Nature communications. 2014; 5:3708.
24. Lakhina V, et al. Netrin/DCC signaling guides olfactory sensory axons to their correct location in the olfactory bulb. The Journal of neuroscience. 2012; 32:4440–56. [PubMed: 22457493]
25. Powell AW, Sassa T, Wu Y, Tessier-Lavigne M, Polleux F. Topography of thalamic projections requires attractive and repulsive functions of Netrin-1 in the ventral telencephalon. PLoS biology. 2008; 6:e116. [PubMed: 18479186]
26. Braisted JE, et al. Netrin-1 promotes thalamic axon growth and is required for proper development of the thalamocortical projection. The Journal of neuroscience. 2000; 20:5792–801. [PubMed: 10908620]
27. Jarjour AA, et al. Maintenance of axo-oligodendroglial paranodal junctions requires DCC and netrin-1. The Journal of neuroscience. 2008; 28:11003–14. [PubMed: 18945908]

28. Rajasekharan S, et al. Netrin 1 and Dcc regulate oligodendrocyte process branching and membrane extension via Fyn and RhoA. Development. 2009; 136:415–26. [PubMed: 19141671]
29. Rabe N, Gezelius H, Vallstedt A, Memic F, Kullander K. Netrin-1-dependent spinal interneuron subtypes are required for the formation of left-right alternating locomotor circuitry. J Neurosci. 2009; 29:15642–9. [PubMed: 20016078]
30. Rabe Bernhardt N, et al. DCC mediated axon guidance of spinal interneurons is essential for normal locomotor central pattern generator function. Developmental biology. 2012; 366:279–89. [PubMed: 22521513]
31. Paul LK, et al. Agenesis of the corpus callosum: genetic, developmental and functional aspects of connectivity. Nat Rev Neurosci. 2007; 8:287–99. [PubMed: 17375041]
32. Jen J, et al. Familial horizontal gaze palsy with progressive scoliosis maps to chromosome 11q23–25. Neurology. 2002; 59:432–5. [PubMed: 12177379]
33. Sabatier C, et al. The divergent Robo family protein rig-1/Robo3 is a negative regulator of slit responsiveness required for midline crossing by commissural axons. Cell. 2004; 117:157–69. [PubMed: 15084255]
34. Zelina P, et al. Signaling switch of the axon guidance receptor Robo3 during vertebrate evolution. Neuron. 2014; 84:1258–72. [PubMed: 25433640]
35. Yu TW, et al. Mutations in WDR62, encoding a centrosome-associated protein, cause microcephaly with simplified gyri and abnormal cortical architecture. Nature genetics. 2010; 42:1015–20. [PubMed: 20890278]
36. Thompson CL, et al. A high-resolution spatiotemporal atlas of gene expression of the developing mouse brain. Neuron. 2014; 83:309–23. [PubMed: 24952961]
37. Lein ES, et al. Genome-wide atlas of gene expression in the adult mouse brain. Nature. 2007; 445:168–76. [PubMed: 17151600]

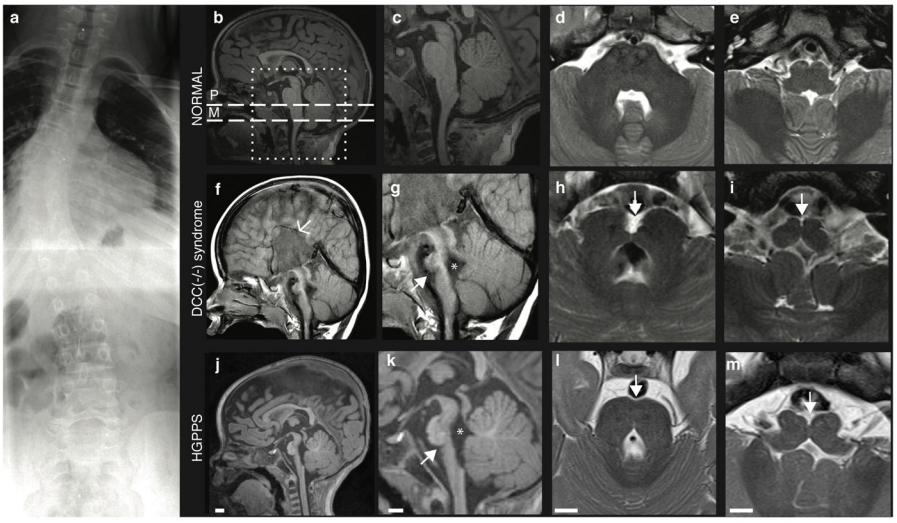

Figure 1. Radiographic features of the *DCC* (−/−) syndrome

(a) Spine film from individual II:7 from Family 1 shows thoracolumbar scoliosis. (b–m) MRI features of affected individual II:2 from Family 2 compared to age matched control and individual with horizontal gaze palsy and progressive scoliosis (HGPPS). (b,f,j) Sagittal images showing agenesis of corpus callosum (arrow) and absent anterior commissure in the affected individual but intact corpus callosum in control and HGPPS individuals. (c,g,k) Zoomed in version (box from Figure 1b) of the sagittal image shows the brainstem abnormalities. The 4th ventricle is enlarged (*). The pons is hypoplastic (arrow) in both affected and HGPPS individuals, but especially in *DCC*(−/−) individuals, with associated elongation of the midbrain and medulla. All are dysmorphic, in particular the pons and midbrain with midline cleft, compared to control. (d,h,l) Axial images through pons (dashed line “P” from Figure 1b) show hypoplasia of the pons and middle cerebellar peduncle and the cleft in the brainstem in the affected and HGPPS individuals (arrow). In addition, the anterior surface of the pons appears irregular (e,i,m) Axial images through medulla (dashed line “M” from Figure 1b) show hypoplasia and “butterfly” appearance of the medulla in the affected and HGPPS individuals (arrow). Scale bars= 1 cm.

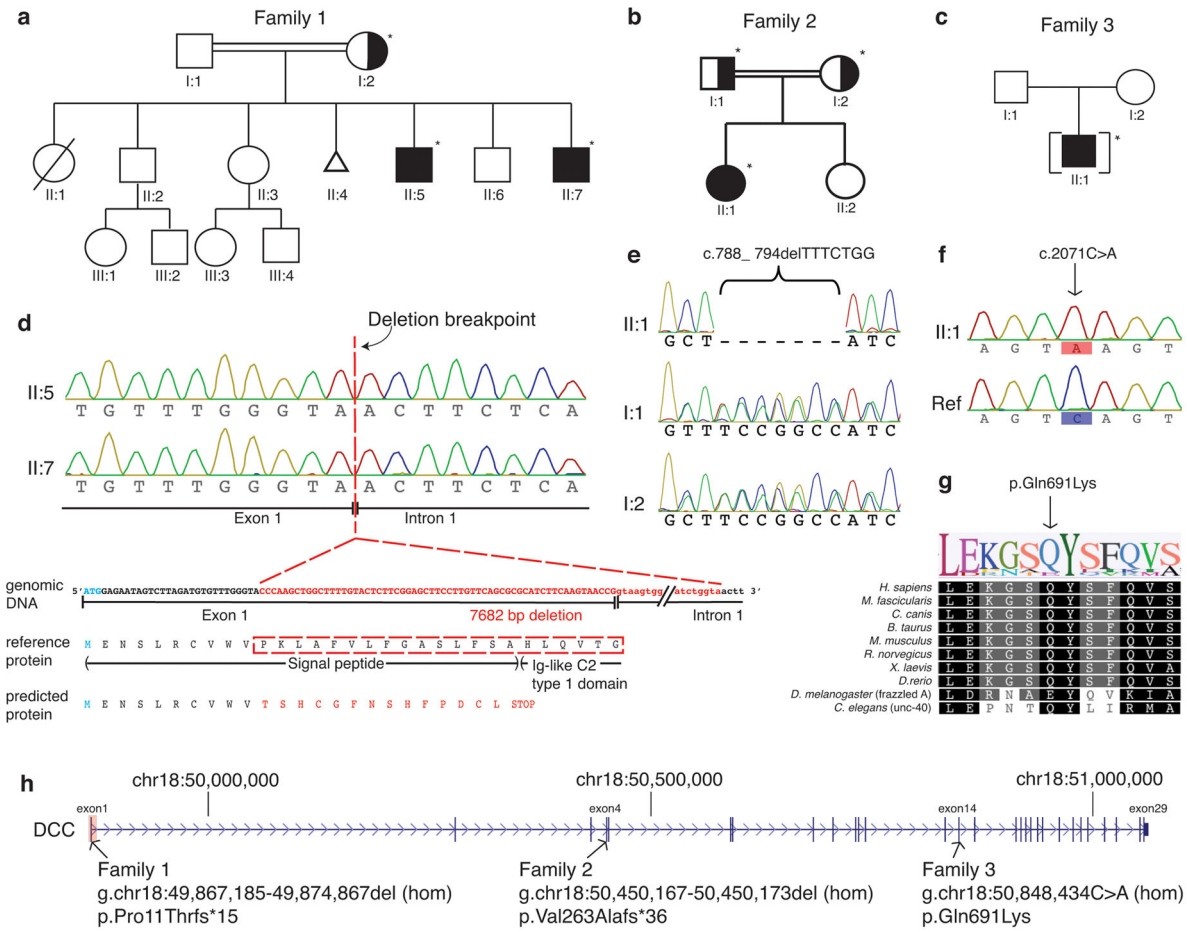

Figure 2. Mapping and identification of mutations in *DCC*

(a–c) Pedigrees of Families 1 (a), 2 (b), and 3 (c). Asterisks indicate family members whose DNA was available (d) Sequencing of the junction PCR products in Family 1 confirmed a 7682 bp intragenic deletion (in red; chr18:49,867,184–49,874,866, hg19 coordinates) that is predicted to result in deletion of 21 amino acids (in grey bar) from the DCC protein, including part of the signal peptide, the Ig-like C2-type 1 domain and the exon 1- intron 1 splice junction. The predicted amino acid sequence also leads to a premature stop codon 15 amino acids downstream from the first changed amino acid. gDNA= genomic DNA, AA= amino acid. M (in blue) indicates translation start site for the predominant isoform of *DCC* (NM_005215.3). (e) Sanger traces from *DCC* sequencing in Family 2 revealed homozygous out-of-frame 7 bp deletion in exon 4 (c.788_794delTTTCTGG) in the proband, and heterozygous deletion in the parents. (f) Sanger trace from *DCC* sequencing in Family 3 revealed a homozygous missense variant NM_005215.3: c.2071C>A; p.Gln691Lys. (g) The residue glutamine (Gln) at position 691 is a highly conserved residue in all species down to *C. elegans,* with the exception of *frazzled* in *D. melanogaster,* which is known to be significantly divergent from other orthologs. (h) Schematic of DCC exon-intron structure with location of the mutations in the three families reported.

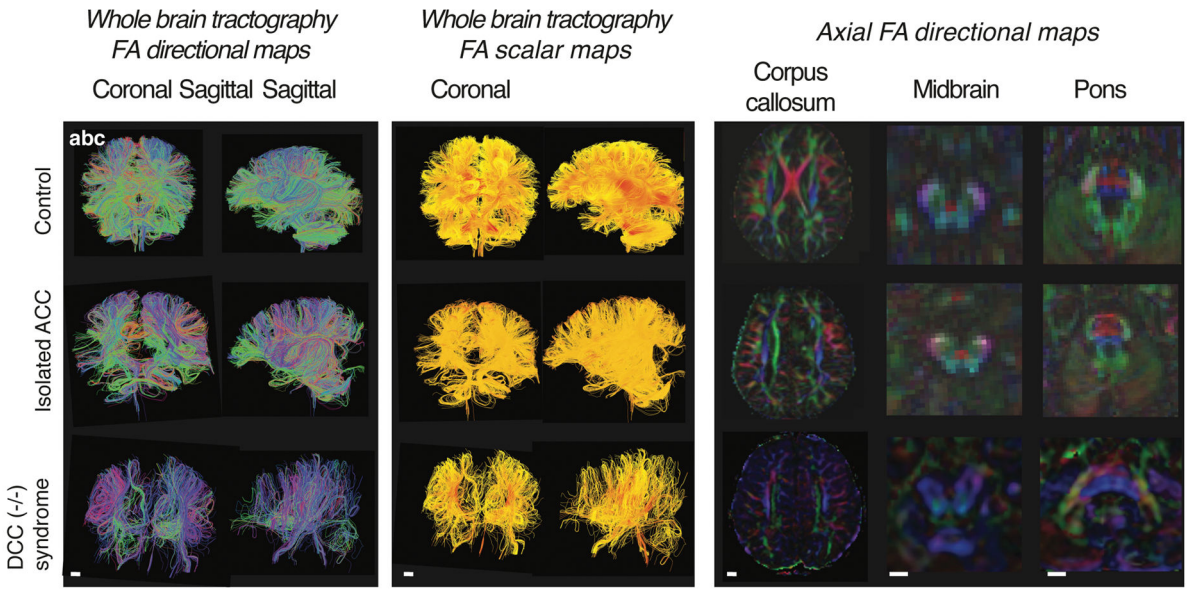

Figure 3. Axon guidance defects in patients with *DCC* (−/−) syndrome

(a,b) Whole brain diffusion tensor tractography (DTT) of control individual, individual with isolated agenesis of the corpus callosum, and individual with *DCC* (−/−) syndrome. (a) Directional maps tracts are pseudocolored to visualize the directions of anisotropic diffusion. Green tracts are going in an anterior posterior direction, red tracts are commissural tracts (left to right), and blue tracts visualize inferior to superior tract directions. Both individuals with ACC and *DCC*(−/−) demonstrate absence of normal interhemispheric commissural fibers. In addition, the *DCC*(−/−) brain exhibits a paucity of reconstructable tracts. (b) Color scalar map is a fractional anisotropy (FA) map, where the scale is a fractional direction scale with units from 0–1. “0” (yellow colored fibers) means the diffusion direction is isotropic, and fibers that are yellow show isotropic diffusion. “1” (red colored fibers) indicate anisotropic diffusion and visualizes fibers where the diffusion is anisotropic. Fibers in the *DCC*(−/−) brain exhibit lower anisotropy and the organization of fibers in general appears disorganized as compared to the control and isolated ACC individuals. (c) Axial FA directional maps of human brain at the levels of the corpus callosum, midbrain, and pons. Both ACC and *DCC*(−/−) brains lack normal crossing fibers (red). In addition, in control and ACC individuals, midbrain color FA maps demonstrate a distinctive “red dot” sign denoting midline decussation of fibers of the superior cerebellar peduncle which are missing from the *DCC*(−/−) brain. Similarly, in the pons, control and ACC individuals exhibit distinct crossing fibers representing midline crossing pontocerebellar fibers; these fibers, too, are missing in the *DCC*(−/−) individual. Scale bars= 1 cm.

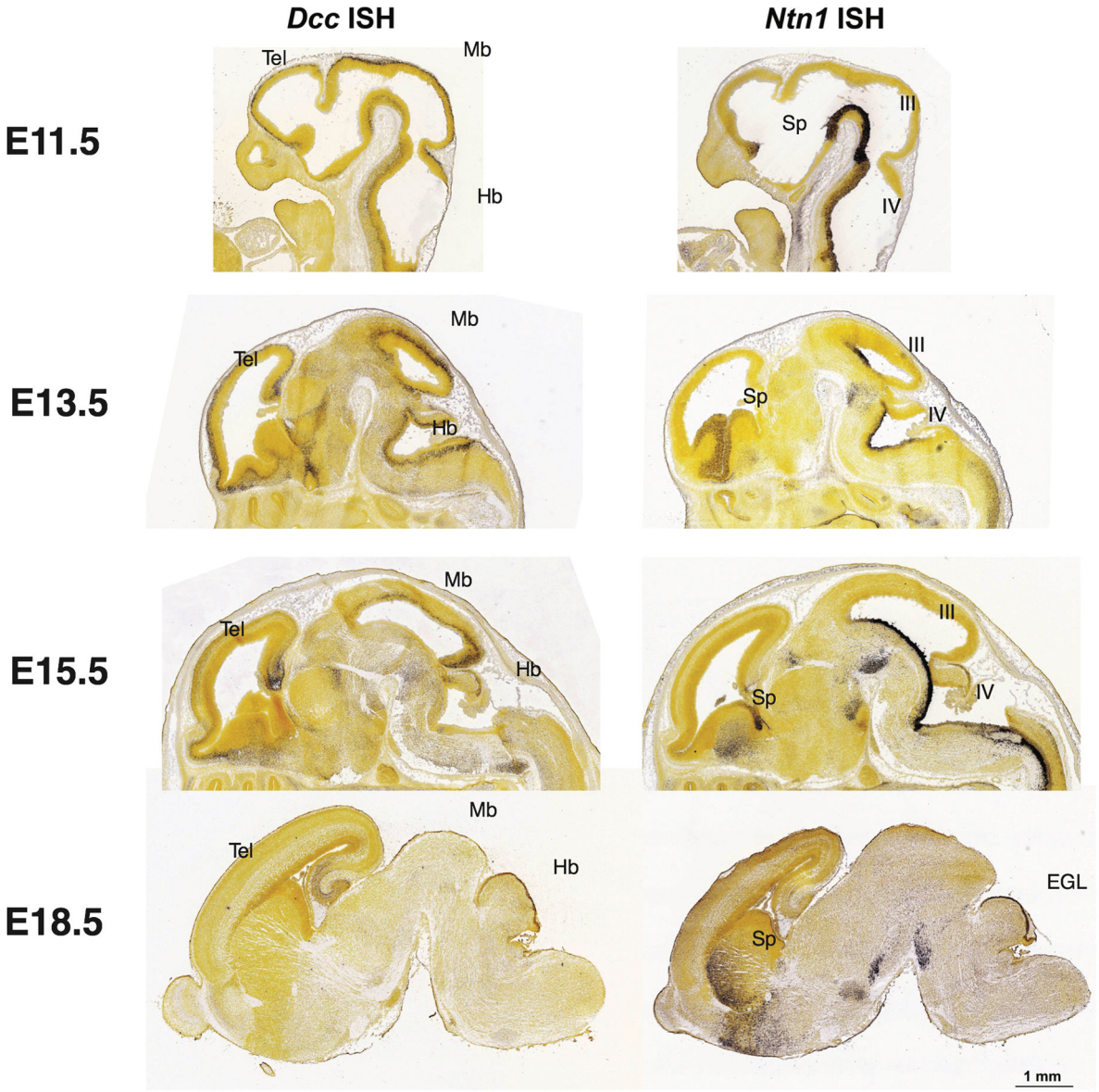

Figure 4. Expression patterns of *DCC* and *Netrin-1* in developing brain

In situ hybridization patterns in E11.5, E13.5, E15.5 and E18.5 mice showing robust early expression in specific, yet largely complementary cell populations in the developing telencephalon, midbrain and hindbrain. *DCC* is particularly highly expressed at early stages in developing neurons of the cortical plate and brainstem nuclei; *DCC* expression subsequently tapers off with age. Similarly, *Ntn* expression is highest in midline structures of the telencephalic expansion and the ventral floor of the developing third and fourth ventricle; its expression also becomes much broader as development proceeds. Tel= telencephalon, Mb= midbrain, Hb= hindbrain, Sp= subpallium, III= third ventricle, IV= fourth ventricle, EGL= external granule layer of cerebellum.

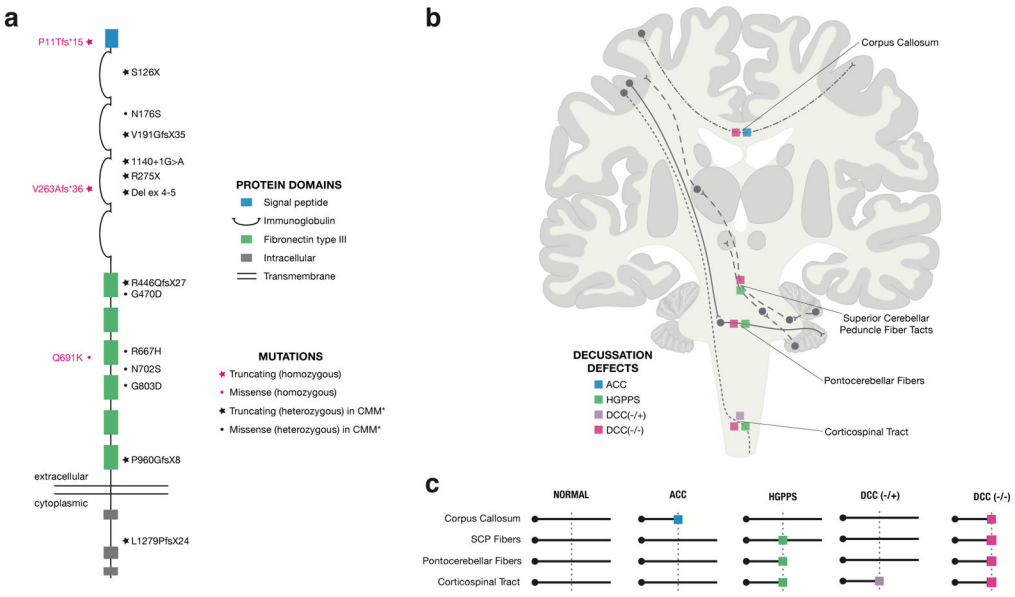

Figure 5. Genotype-phenotype correlations in *DCC* and other related disorders of midline axon guidance

(a) *Structure of the DCC protein and location of the DCC mutations* identified in our report (in magenta) and in congenital mirror movements (in black). *DCC* encodes a transmembrane receptor with four immunoglobulin and six fibronectin type III domains, and three conserved cytoplasmic domains. In Family 1, homozygous loss of exon 1 results in a deletion of the signal peptide, as well as the first immunoglobulin-like C2 domain, and is predicted to lead to a nonfunctional protein. In Family 2, homozygous frameshift in exon 4 is predicted to lead to a nonfunctional protein. In Family 3, the missense mutation (Gln691Lys) affects the third fibronectin type III domain. Individuals with congenital mirror movements have truncating heterozygous mutations in *DCC*; however, these individuals have normal brain MRI and normal intellect. (b,c) *Major tract abnormalities in the DCC (−/−) syndrome and other human disorders of axon guidance:* Anatomical schematic of the ACC (blue box) vs. HGPPS (green box) vs. *DCC* (−/+) (purple box) vs. *DCC* (−/−) (magenta box) mutant phenotypes (C) and summary schematic (D) depicting disruptions in different commissural tracts in each disorder. In ACC, only supratentorial tracts are affected, while HGPPS affects only infratentorial tracts. In DCC (−/+), corticospinal tracts are functionally disrupted. In *DCC* (−/−), midline crossing along the entire length of the neuraxis is disrupted. ACC= agenesis of corpus callosum, HGPPS= horizontal gaze palsy with progressive scoliosis.